Quantum Fourier Transform to Estimate Drive Cycles

Vinayak Dixit (v.dixit@unsw.edu.au)
UNSW Sydney
Sisi Jian
the Hong Kong University of Science and Technology

Research Article

Keywords: Drive cycles, Quantum Fourier Transform, vehicle systems, energy consumption, emissions

Posted Date: August 4th, 2021

DOI: https://doi.org/10.21203/rs.3.rs-772223/v1

Quantum Fourier Transform to Estimate Drive Cycles

Vinayak Dixit[a*], Sisi Jian[b]

a Research Centre for Integrated Transport Innovation (rCITI), School of Civil and Environmental Engineering, UNSW Sydney
b Department of Civil and Environmental Engineering, the Hong Kong University of Science and Technology, Clear Water Bay, Kowloon, Hong Kong SAR, China

*Corresponding author, Tel: (+61 2) 9385 5721, Email: v.dixit@unsw.edu.au

Quantum Fourier Transform to Estimate Drive Cycles

Abstract

Drive cycles in vehicle systems are important determinants for energy consumption, emissions, and safety. Estimating the frequency of the drive cycle quickly is important for control applications related to fuel efficiency, emission reduction and improving safety. Quantum computing has established the computational efficiency that can be gained. A drive cycle frequency estimation algorithm based on the quantum Fourier transform is exponentially faster than the classical Fourier transform. The algorithm is applied on real world data set. We evaluate the method using a quantum computing simulator, demonstrating remarkable consistency with the results from the classical Fourier Transform. Current quantum computers are noisy, a simple method is proposed to mitigate the impact of the noise. The method is evaluated on a 15 qbit IBM-q quantum computer. The proposed method for a noisy quantum computer is still faster than the classical Fourier transform.

1. Introduction

Drive cycles are important determinants of emissions, energy consumption and safety. Higher frequencies of acceleration and deceleration cycles are predictors of higher emissions, fuel consumption (Ligterink et al. 2012) and crashes (Dixit et al., 2011; Dixit, 2013). Regulators, vehicle manufacturers and traffic engineers are extremely interested to understand the driving cycles for implementing policies and real-time control systems.

Current vehicle systems rely on Fourier Transformation to evaluate the frequency domain for vehicle control. This study demonstrates the use of a Quantum Fourier Transform to extract the frequency domain. Which could have significant implications on ability to react faster to improve safety, fuel efficiency and reduce emissions (Figure 1).

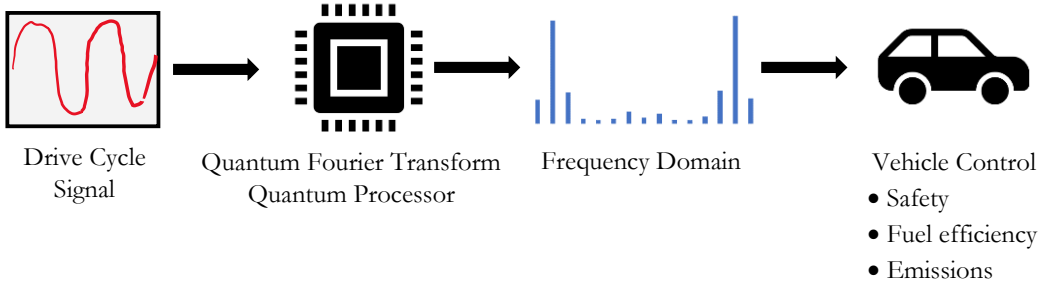

Figure 1: Quantum Fourier Transform for Drive Cycle Analysis

Research in quantum computing and algorithms over the past three decades have theoretically demonstrated the potential gains through "quantum speedup" (Montanaro, 2016). At a fundamental level, quantum computers differ from classical computers in their ability to leverage quantum mechanical properties such as superposition, entanglement and interference to speedup computations.

Applications of quantum algorithms in the field of transportation and traffic have been limited. Bernas and Wisniewska (2013), provided a preliminary framework for expressing a Cellular Automata Traffic Model in a Quantum Computable Format. Though the initial approach is interesting, there are significant issues for scaling their proposed approach. Their approach required $N \log_2 S$ number of qubits, where N is the number of vehicles and S the number of road sections. Even a modest network of 1000 vehicles and 64 road sections, would require 6000 qubits, which would be extremely cost prohibitive.

D-Wave quantum computers (https ://www.dwavesys.com/) are essentially a very different quantum computational engine. They rely on the process of "Quantum annealing" to start from a particular system state to that of the final state defined by a Hamiltonian defining the feasible states. As is well known, finding minimum energy states in non-convex Hamiltonians is an NP-hard problem that classical computers take long to solve. The fundamental physical nature of the D-Wave quantum computer makes them feasible to solve an Ising model that is isomorphic to a Quadratic Unconstrained Binary Optimization (QUBO) Problem.

This led to a significant foray into representing some of the transportation problems as a QUBO problem, that could be solved on a D-Wave. These include (a) Travelling Salesman Problem, that has been thoroughly reviewed and evaluated by Warren (2020) (b) Travelling Salesman Problem with Time Windows (Papalistas et al. 2020) (c) Vehicle Routing Problems as well as its variants such as multi-depot capacitated vehicle routing problem (MDCVRP) and its dynamic version (Harikrishnakumar et al. 2020) (d) Traffic signal control (Hussain et al. 2020), and (e) Redistributing and rerouting vehicles for optimal network utilization (Neukart et al. 2017). It is important to note that Quantum annealing is a meta-heuristic (Kadowaki and Nishimori, 1998), though it has repeatedly demonstrated to out-perform classical computers to get to more efficient solutions quicker, they do not guarantee optimality until exhausting the search space. Even though quantum computers might outperform classical computers by orders of magnitude, Aaronson (2008) identified NP-Complete problems as one of the limits of Quantum Computers.

Though meta-heuristic approaches are useful, the field of transportation management, policy and planning are subject to scrutiny. This is predominantly because of the safety critical aspects as well as the wide public impact transport interventions have on society. This requires providing structural bounds and assurances on the validity of the solution. This need from a decision support standpoint requires to rely on quantum logic gates.

There has been ground breaking theoretical work that demonstrated quantum algorithms relying on quantum logic gates can provide significant speedups, to name a few: (a) Deutsh-Jozsa algorithm (Deutsch and Jozsa, 1992) to determine constant of symmetric output provides exponential speedup (b) Simon's period finding algorithm (Simon, 1994) provides exponential speedup (c) Bernstein-Vazirani secret string determination algorithm (Bernstein and Vazirani, 1997) provides super-polynomial speedup (d) Grover's search Algorithm (Grover, 1997) provides quadratic speedup and (e) Dürr-Høyer algorithm (Dürr and Høyer, 1996) to find minimum provided polynomial speedup. One of the most celebrated is the Shor's (1994) algorithm, that demonstrated that quantum computers can solve the prime factorization problem exponentially faster than classical computers, having significant implications on cryptography. Though subject to some debate, recently "Quantum Supremacy" was demonstrated on a problem that would take a classical supercomputer 10,000 years to be completed by 53 qubit Sycamore processor in 200 seconds (Arute et al. 2019).

This research contributes by implementing a Quantum Fourier Transform (QFT) to evaluate the frequency domain of the drive cycle. The validity of this method is demonstrated using the IBM(https://quantum-computing.ibm.com/) quantum simulator. The QFT algorithm is also implemented on IBM's freely available IBM-Q16 Melbourne, that can be used to create a 15-qubit quantum circuits. The IBM-Q16 does not have a full error correction capability, resulting in noisy outputs. A simple error correction method is proposed that does not compromise the quantum speedups.

2. Quantum Circuits

Basic information of qubits, Quantum Circuits and Quantum Fourier Transform are detailed, to provide completeness for broader transportation and traffic researchers. For further details, please refer to Nielsen and Chuang (2011). Qubits are the basic unit of quantum information in a quantum circuit. A

qubit is represented as a linear superposition of its two orthonormal vectors. These vectors are usually denoted as,

$$|0\rangle = \begin{bmatrix}1\\0\end{bmatrix} \text{ and } |1\rangle = \begin{bmatrix}0\\1\end{bmatrix} \quad [1]$$

Therefore, a qubit can be represented as a linear combination of $|0\rangle$ and $|1\rangle$:

$$\varphi = \alpha|0\rangle + \beta|1\rangle \text{ Where } |\alpha|^2 + |\beta|^2 = 1 \quad [2]$$

It should be noted that α and β are complex valued and the corresponding probability amplitudes for $|0\rangle$ and $|1\rangle$. This means that we can measure $|0\rangle$ with a probability of $|\alpha|^2$ and $|1\rangle$ with a probability of $|\beta|^2$. The concept of "superposition" implies that there is no way to tell which of the two possible states the qubit is in. In fact, the moment we measure a qubit, it collapses to the measured state. As you will see later the probability amplitudes are responsible for quantum "interference".

A quantum circuit is a sequence of quantum gates that carry out the computation by operating on the qubits. Quantum gates are Unitary operators (U, i.e. $UU^\dagger = I$), and therefore a quantum circuit is reversible.

Quantum algorithms begin with creating a superposition of qubits that act as an input for the quantum oracle function (U_f), which is a quantum version of the classical function (f). This process is referred to as "quantum parallelism", which is widely used as a starting point to build useful quantum algorithms.

2.1 Discrete Fourier Transforms

As quantum fourier transform is a quantum implementation of the classical fourier transform. Therefore, it is critical to provide a brief overview of a Discrete Fourier Transform (DFT). DFT acts on a complex valued vector $(x_0, x_1, \dots x_{N-1})$ to transform it into another complex valued vector $(y_0, y_1, \dots y_{N-1})$ according to the formula:

$$y_k = \frac{1}{\sqrt{N}} \sum_{j=0}^{N-1} x_j e^{2\pi i \frac{jk}{N}} \quad [3]$$

If x_j has a period τ, then y_k is non-zero for k that are multiples of N/τ. Else, it is zero everywhere else. The magnitude of the coefficients of the fourier basis indicate the amount of that frequency carried in the signal. Therefore, a Fourier transforms a series from the time domain to the frequency domain, making it possible to infer the frequency spectrum. The Fast Fourier Transform is known to have a time complexity of $\mathrm{O}(N \log N)$.

2.2 Quantum Fourier Transforms

To employ QFT, we need to define an n-qubit quantum states as inputs, s.t. $N = 2^n$. The QFT transforms x_i to the fourier coefficients y_i.

$$\sum_{i=0}^{N-1} x_i |i\rangle \xrightarrow{QFT} \sum_{i=0}^{N-1} y_i |i\rangle \quad [4]$$

It is important to note that the probability of measuring state $|i\rangle$ in the standard basesis will be $|y_i|^2$. Therefore, applying QFT to a periodic function with period τ, would result in a high likelihood of the measurement of $|k\rangle$, when k is a multiple of N/τ. If τ does not perfectly divide N, then as in the case of the fourier transform, there will be measurements in the neighbourhood of the multiple of N/τ

A QFT is implemented on a vector of length $N = 2^n$, represented by a basis state by $|x\rangle = |x_1\rangle \otimes |x_2\rangle \otimes \dots \otimes x_n$ and $x = 2^{n-1}x_n + \cdots + 2x_1 + x_0$.

$$QFT_N|x\rangle = \frac{1}{\sqrt{N}} \sum_{y=0}^{N-1} e^{2\pi i \frac{xy}{2^n}} |y\rangle \quad [5]$$

$$QFT_N|x\rangle = \frac{1}{\sqrt{N}} \sum_{y=0}^{N-1} e^{2\pi i \frac{x \sum_{k=1}^{n} 2^{n-k} y_k}{2^n}} |y_1, y_2 \dots y_n\rangle \quad [6]$$

$$QFT_N|x\rangle = \frac{1}{\sqrt{N}} \sum_{y=0}^{N-1} \prod_{k=1}^{n} e^{2\pi i x y_k / 2^k} |y_1, y_2 \dots y_n\rangle \quad [7]$$

After rearranging the sum and products we get entangled states

$$QFT_N|x\rangle = \frac{1}{\sqrt{N}} \otimes_{k=1}^{n} (|0\rangle + e^{\frac{2\pi i x}{2^k}} |1\rangle) \quad [8]$$

$$QFT_N|x\rangle = \otimes_{k=1}^{n} \frac{1}{\sqrt{2}} (|0\rangle + e^{2\pi i x / 2^k} |1\rangle) \quad [9]$$

$$QFT_N|x\rangle = \otimes_{k=1}^{n} \frac{1}{\sqrt{2}} (|0\rangle + e^{2\pi i \sum_{j=1}^{k} x_{n+1-i}/2^i} |1\rangle) \quad [10]$$

2.3 Quantum Fourier Circuit

A quantum circuit to undertake QFT relies on three types of gates (a) Hadamard Gate (b) $CROT_k$ Gate, and (c) Swap Gate. The matrix operations for these three gates are shown in Equations 11-18, and the circuit representations are shown in Figure 2.

The Hadamard Gate transforms a qubit x_k

$$H = \frac{1}{\sqrt{2}} \begin{bmatrix} 1 & 1 \\ 1 & -1 \end{bmatrix} \quad [11]$$

$$H|x_k\rangle = \frac{1}{\sqrt{2}} (|0\rangle + e^{\frac{2\pi i x_k}{2}} |1\rangle) \quad [12]$$

The two-qubit controlled rotation $CROT_k$ gate is defined by

$$CROT_k = \begin{bmatrix} I & 0 \\ 0 & UROT_k \end{bmatrix} \quad [13]$$

$$UROT_k = \begin{bmatrix} 1 & 0 \\ 0 & e^{\frac{2\pi i}{2^k}} \end{bmatrix} \quad [14]$$

$$CROT_k|0x_i\rangle = |0x_i\rangle \quad [15]$$

$$CROT_k|1x_i\rangle = e^{\frac{2\pi i x_i}{2^k}} |1x_i\rangle \quad [16]$$

The $SWAP$ gate is defined by

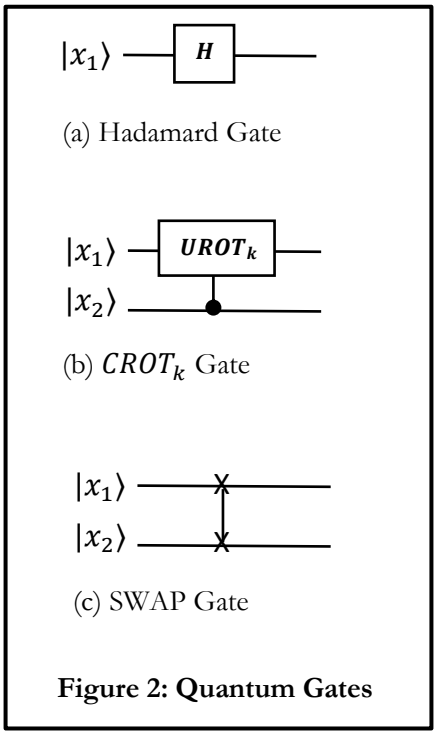

(a) Hadamard Gate

(b) $CROT_k$ Gate

(c) SWAP Gate

Figure 2: Quantum Gates

$$SWAP = \begin{bmatrix} 1 & 0 & 0 & 0 \\ 0 & 0 & 1 & 0 \\ 0 & 1 & 0 & 0 \\ 0 & 0 & 0 & 1 \end{bmatrix} \quad [17]$$

$$SWAP|x_i x_j\rangle = |x_j x_i\rangle \quad [18]$$

A full algorithm to determine the QFT starts with an n-qubit input state $|x_1 x_2 \dots x_n\rangle$. The corresponding full quantum circuit is shown in Figure 2.

(1) A Hadamard gate is applied on qubit 1, and the state is transformed from the input state to:

$$H_1|x_1 x_2 \dots x_n\rangle = \frac{1}{\sqrt{2}}[|0\rangle + e^{\frac{2\pi i x_1}{2}}|1\rangle] \otimes |x_2 x_3 \dots x_n\rangle \quad [19]$$

(2) Then apply $CROT_k$ in series controlled by qubit $k = 2 \dots n$. This results in:

$$\frac{1}{\sqrt{2}}[|0\rangle + e^{\frac{2\pi i x_1}{2}+\frac{2\pi i x_2}{4}\dots+\frac{2\pi i x_n}{2^n}}|1\rangle] \otimes |x_2 x_3 \dots x_n\rangle \quad [20]$$

(3) Recursively applying Steps (1) and (2) on qubits $i = 2..n$.

(4) Then apply swap gates to reverse the order of the qubits, to get

$$\otimes_{k=1}^{n} \frac{1}{\sqrt{2}}(|0\rangle + e^{2\pi i \sum_{j=1}^{k} \frac{x_{n+1-i}}{2^i}}|1\rangle) \quad [21]$$

(5) Measure the n-qubits.

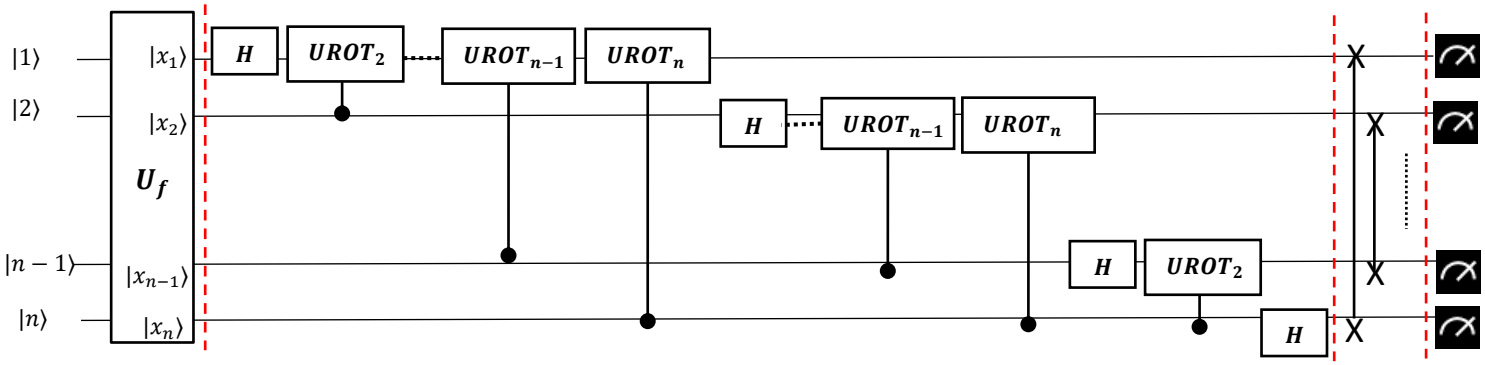

Figure 3: Circuit for a Quantum Fourier Transform

As can be seen in the circuit shown in Figure 3. The first qubit would require n gates, i.e. one Hadamard gate and $n-1$ $UROT$ gates. A generic qubit k would require $n-k+1$ gates. Followed by $n/2$ swap gates. Therefore, the total number of operations required will be $\left(\frac{n}{2} + \sum_{k=1}^{n} n-k+1\right) = \frac{n^2}{2} + n$. Hence the complexity of QFT is $O(n^2)$ or $O((\ln N)^2)$, which is an exponential improvement over a Fast Fourier Transformation. This is a well-known result and is discussed in detail in Nielsen and Chuang, 2010).

We demonstrate the application through simulations and implementation on the IBMq16-Melbourne, quantum computer. This is the first application of quantum computing to study traffic dynamics data, particularly in the context of evaluate drive cycles.

3. Drive Cycle Data

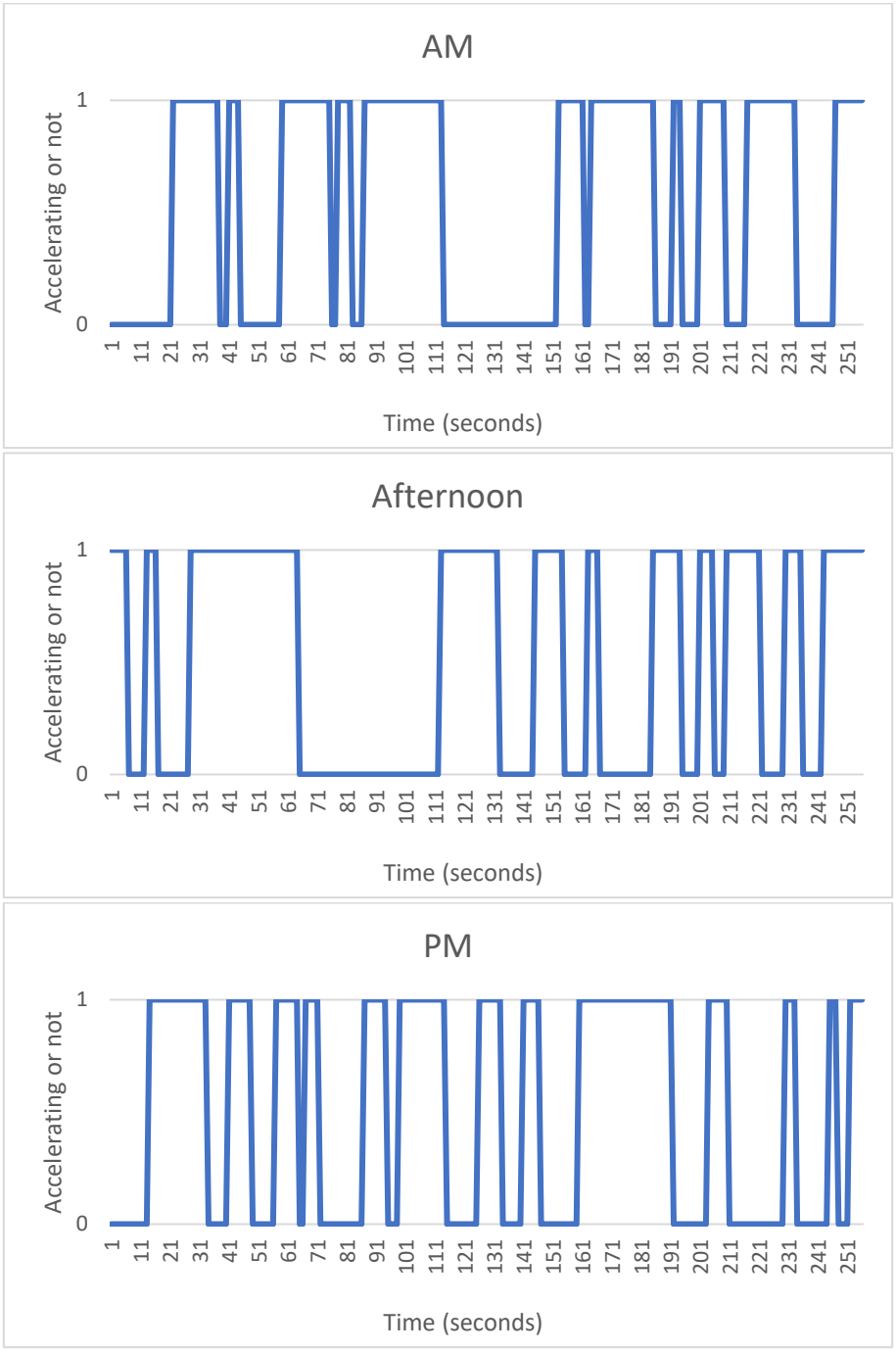

Figure 4: Time series acceleration data.

The National Renewable Energy Laboratory (NREL) publishes drive cycle data that include second-by-second data on the vehicles speed and accelerations using a global positioning system(https://www.nrel.gov/transportation/secure-transportation-data/tsdc-drive-cycle-data.html). This acceleration data was used to create a binary variable indicating whether the vehicle was accelerating or decelerating to create a time series comprising of a sequence of binary numbers.

CALTRANS data from 27th Nov 2012 was used during the following time periods (a) 8:42AM-8:47AM (120-420) (b)13:07PM-13:32PM (15969-17512), and (c) 18:37-19:04-(35770-37411). The time series data for the acceleration and deceleration during these three time periods are shown in Figure 4.

4. Comparison of Quantum Fourier Transform with Classical Fourier Transform

The Quantum Fourier Transform circuit discussed was setup to analyse the frequency domain of the acceleration-deceleration cycles for a 256 second time period. The circuit was run using the IBM Quantum Simulator. The spectral data obtained from the quantum Fourier transform and the Fourier transform are in close agreement as seen in Figure 5. A perfect correlation (correlation coefficient~1) was observed between the square root of the probabilities estimated from the QFT and the coefficients of the Fourier Transform (See Figure 6).

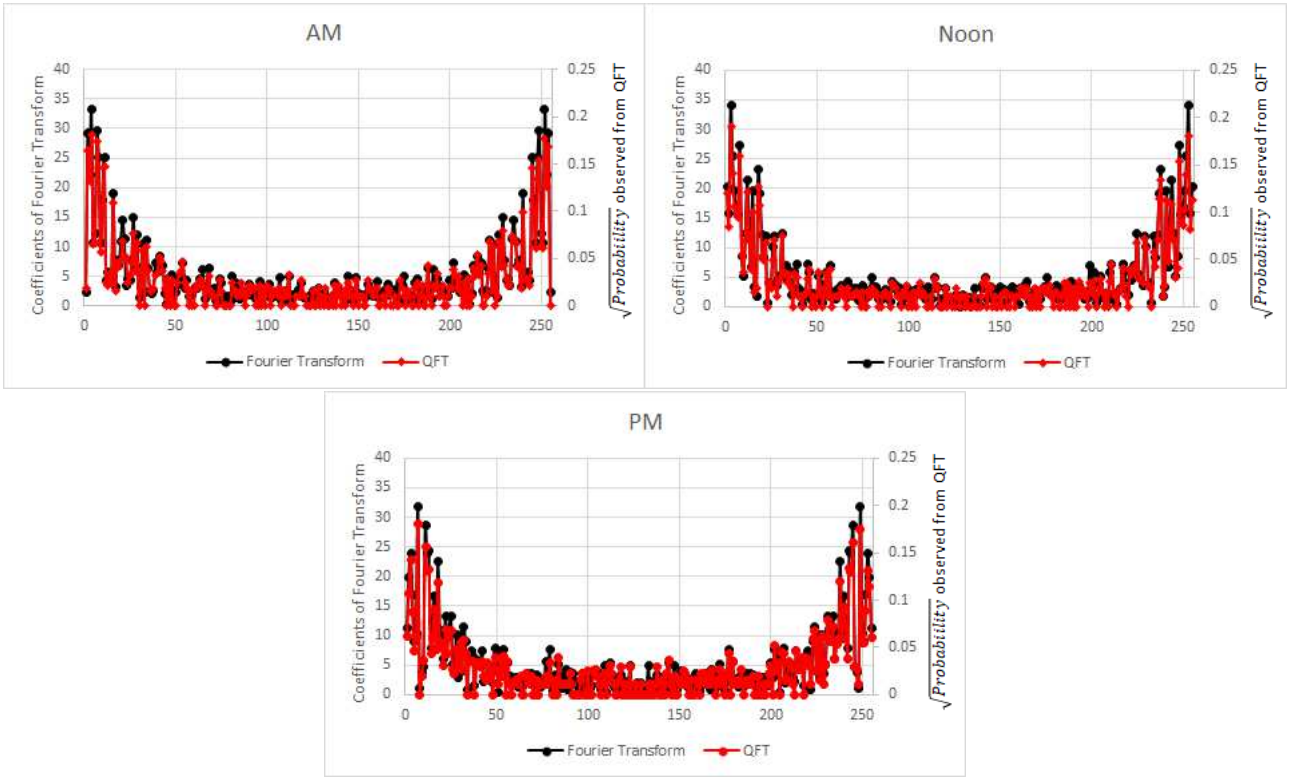

Figure 5: Comparison of the frequency domain based on calculations from QFT and Fourier Transform

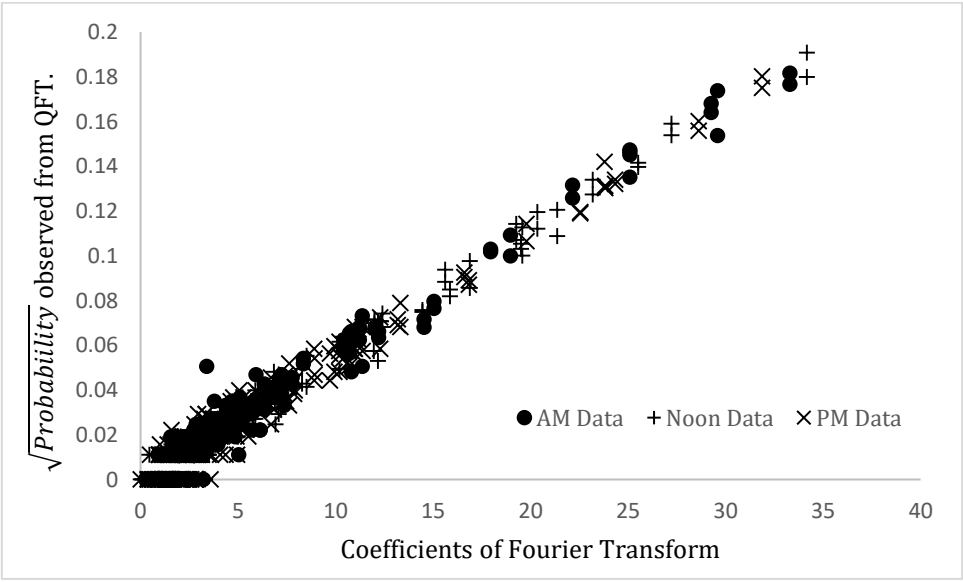

Figure 6: Comparison of the coefficients of the Fourier Transform and QFT

5. QFT using Noisy Quantum Computing

Due to the extreme difficulty in controlling the qubits, current Quantum Computing Technology tend to be noisy with a small probability of an error in the qubit. Methods to correct these errors are required to develop applications using Noisy Intermediate-Scale Quantum Computing (NISQ) (Preskill, 2019).

The 15 qubit IBM-Q16 Melbourne computer was used for this analysis. This limited the length of the sequence of data on which the quantum Fourier transform can be calculated to be 16. To conduct this analysis, sixteen series of baseline sequences were generated which will be referred to as the calibrating dataset and six sequences were randomly generated and are referred to as the evaluation dataset. These were used to calibrate for the underlying error structure and evaluate the error model.

The probabilities observed from the IBM-Q16 Melbourne were compared with the probabilities generated from the IBM quantum simulator. The comparison between the observed and actual probabilities are shown in Figure 7a. Though there is a discernible positive correlation of 0.34* (statistically significant at a 99 percent confidence), there is significant noise that is observed.

A deeper analysis, comparing the observed probabilities with the when the actual probabilities were zero is shown in Figure 7b. Other than the consistent bias in the observed probabilities being greater than zero, the magnitude in level of bias varies between the different values in the frequency domain.

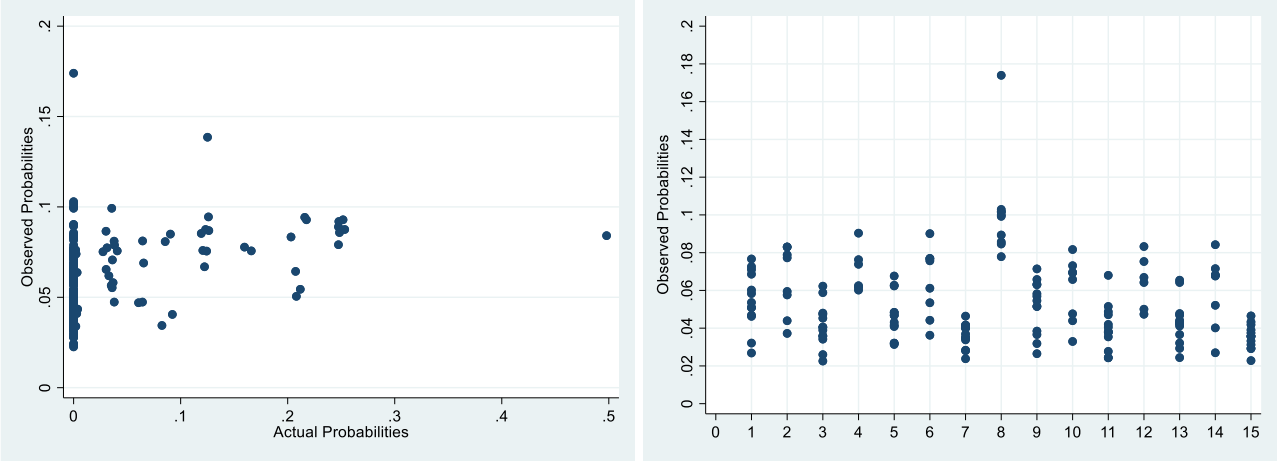

Figure 7: Calibration Data (a) Observed vs Actual Probabilities (b) Spectral analysis of the observed probabilities when actual probabilities is zero.

As discussed earlier, the QFT implemented on a vector represented by $x = 2^{n-1}x_n + \cdots + 2x_1 + x_0$, results in a probability (P_y) of observing y in the Fourier domain measured as $y = 2^{n-1}y_n + \cdots + 2y_1 + y_0$. In a noisy quantum computer, the transformation in Equation 4 occurs with errors, assuming that there are independent errors for each *y*, P_y^{ϵ}. Therefore, the observed probabilities $P_{y\epsilon}$ can be written as a function of the actual probabilities P_y and the probability of deviating from *y*, that is P_y^{ϵ} (Equation 22).

$$P_{y\epsilon} = P_y\left(1 - P_y^{\epsilon}\right) + (1 - P_y)P_y^{\epsilon}$$

$$P_{y\epsilon} = P_y + P_y^{\epsilon} - 2P_yP_y^{\epsilon} \qquad [22]$$

We use the calibration dataset to determine the error probability (P_y^{ϵ}) in Equation 22. The actual probabilities were estimated using the simulator and the observed probabilities were determined using the IBMQ-16 Melbourne quantum computer. As $P_{y\epsilon}$ and P_y are known for each *y*, P_y^{ϵ} was estimated by regressing between the observed and actual probabilities for each *y* (See Figure 8).

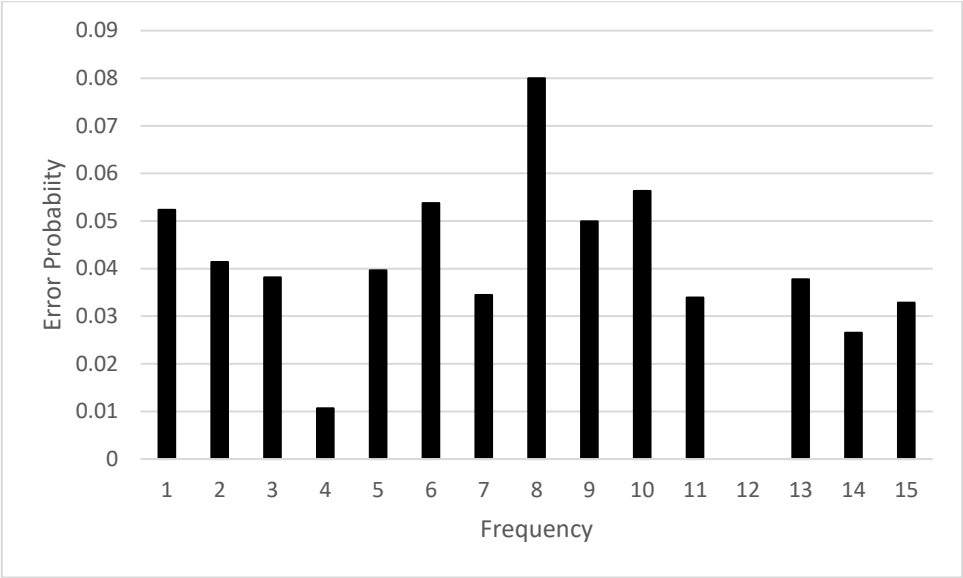

Figure 8: Error probabilities for each frequency value

The actual probability P_y can be estimated by Equation 23.

$$\widehat{P_y} = \frac{P_{y\epsilon} - P_y^{\epsilon}}{1 - 2P_y^{\epsilon}} \qquad [23]$$

Furthermore, the probability distribution of the observed probabilities when the actual probabilities are zero was found to have a median of 0.051 and the 95th percentile value of 0.089 (See Figure 9). If the observed probability is less than 0.089, it would not be possible to distinguish if the observed probability appears because the actual probabilities are zero or not. Therefore, in the evaluation only observed probabilities are greater than the 95th percentile value of 0.089 are considered. This is denoted by $P_{y\epsilon}^{95}$.

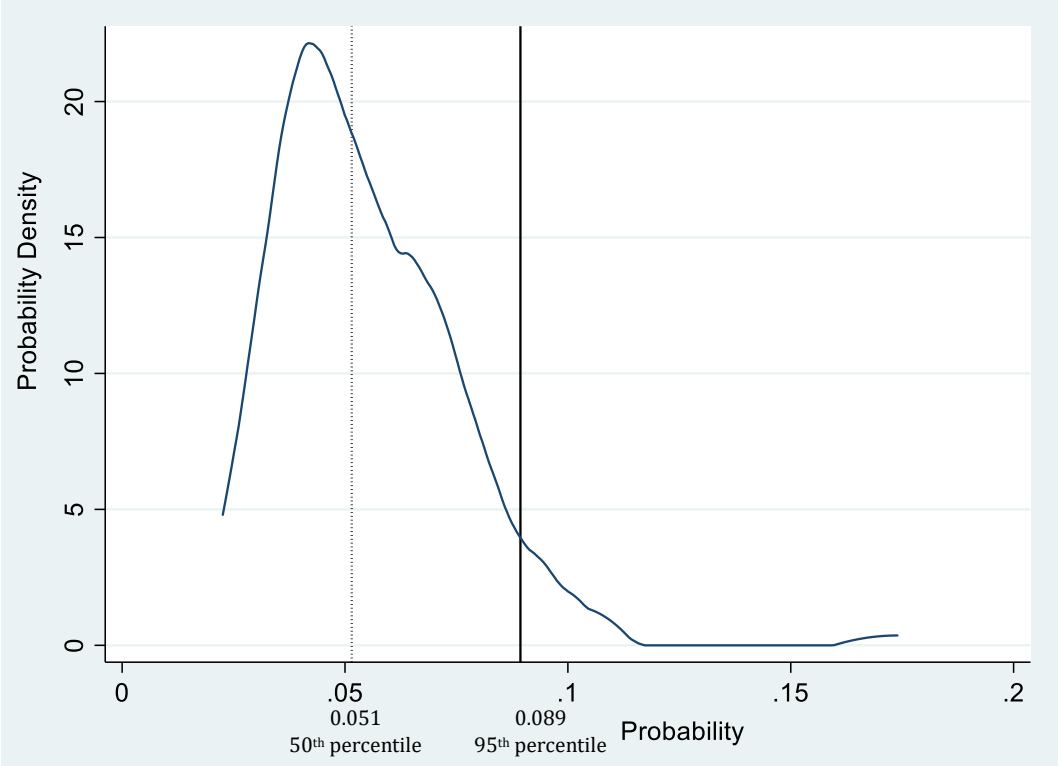

Figure 9: The probability density of the observed probabilities when actual probabilities is zero.

The estimated probabilities (Figure 10) align closely with the actual probabilities (correlation of 0.86), as compared to the observed probabilities (correlation of 0.59).

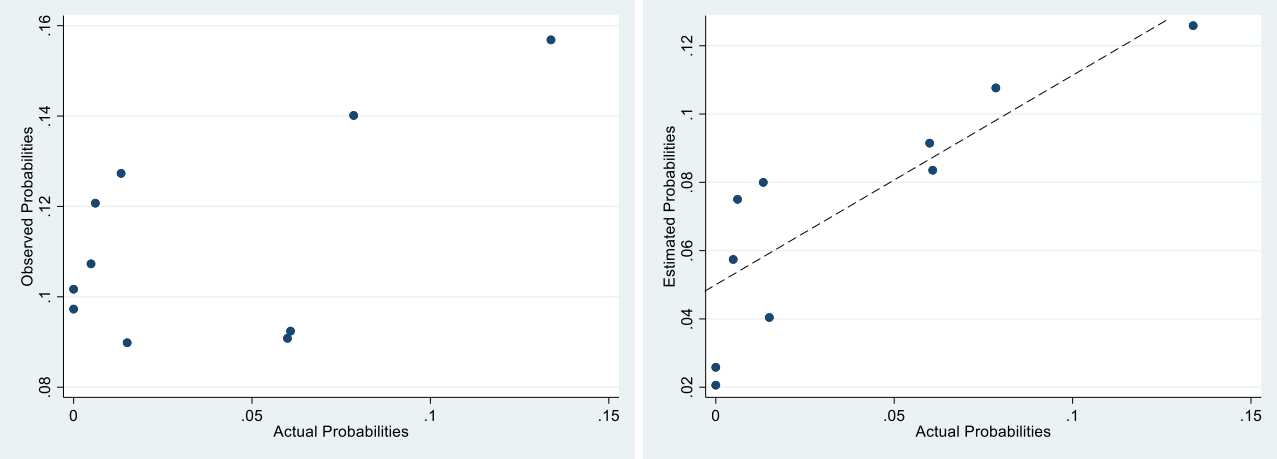

Figure 10: Comparing (a) Observed and actual probabilities (b) Estimated and actual probabilities

Figure 11 summarizes the overall method in a flow chart. The proposed method using a NISQ based computing system only requires the calibrated error probability (P_y^{ϵ}) and the observed probability ($P_{y\epsilon}^{O}$), therefore it takes a single step to determine the accurate probabilities. Therefore, the computational complexity of post processing to determine the dominant frequency is still $O((\ln N)^2)$. It should be however noted that the dominant frequency needs to have the observed probabilities greater than the threshold ($P_{y\epsilon}^{95}$). This limits the applications of this method to use cases where the frequencies have observed probabilities greater than the thresholds.

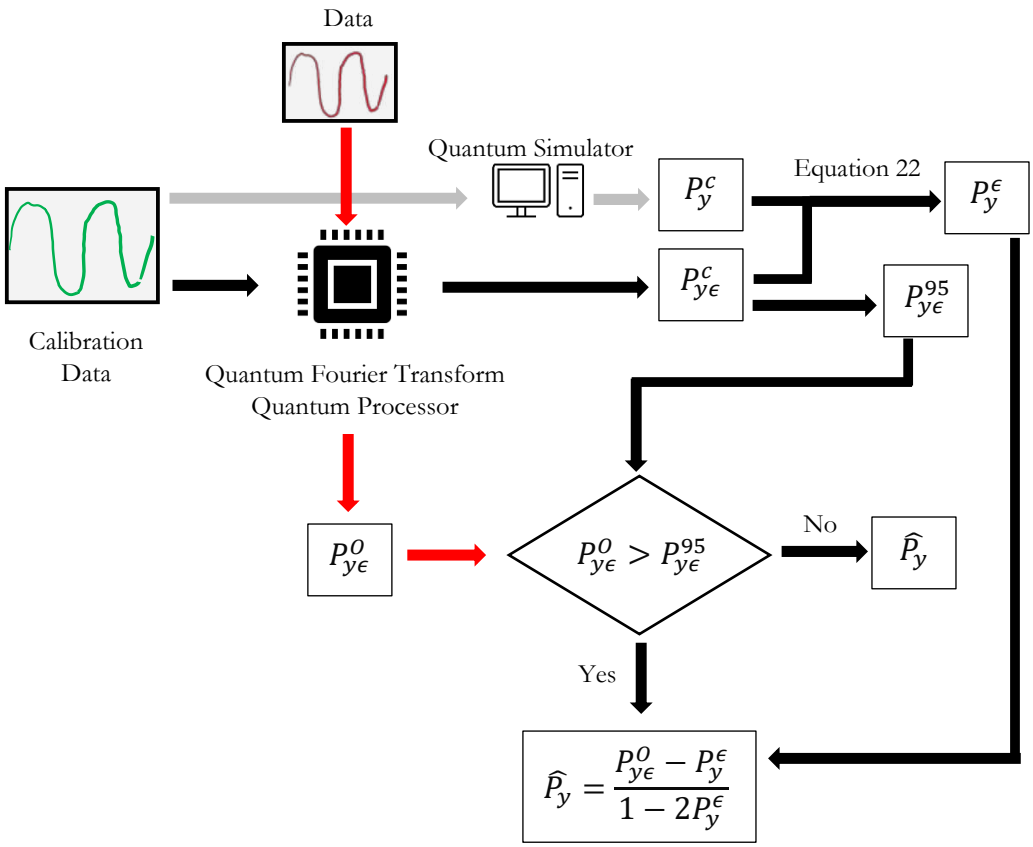

Figure 11: Flow chart of method to estimate probabilities using NISQ

6. Conclusion

This paper is one of the first to explore the use of quantum computing for vehicle dynamics and drive cycle analysis. The method particularly relies on the Quantum Fourier Transform (QFT) that is known to be exponentially faster than the Fourier Transform to determine dominant Drive Cycle frequencies.

Using the IBM Quantum Computing Simulators, the study was able to demonstrate that the implementation of the QFT for drive cycle analysis was consistent with the results from the classical Fourier Transform.

Current quantum computers are known to have errors, and in the era of NISQ, it is imperative to develop methods that can achieve quantum speedups despite these errors. The study proposed a simple error correction method to estimate the probabilities consistent with QFT, without compromising the computational complexity. The method was able to reasonably well recover the probabilities.

We are embarking on an exciting frontier of quantum computing that has significant implications on vehicle dynamics, transportation planning and traffic management. These could help with identifying issues quickly and rapidly determining optimal responses, which could in turn help reduce congestion, emissions and improve safety.

7. References

1. Aaronson, S. (2008) "The Limits of Quantum" Scientific American 298(3):50-7.
2. Arute, F., Arya, K., Babbush, R. et al. (2019). Quantum supremacy using a programmable superconducting processor. Nature 574, 505–510.
3. Bernas, M. and Wisniewska, J. (2013) "Quantum Road Traffic Model for Ambulance Travel Time Estimation" Journal of Medical Informatics and Technologies, Vol. 22/2013, ISSN 1642-6037
4. Bernstein, E. and Vazirani, U. (1997). Quantum Complexity Theory. SIAM Journal on Computing. 26 (5): 1411–1473.
5. Deutsch, D. and Jozsa, R. (1992). Rapid solutions of problems by quantum computation. Proceedings of the Royal Society of London A. 439 (1907): 553–558.
6. Dixit, V.V.; Pande, A.; Abdel-Aty, M.; and Radwan, E. (2011). Quality of traffic flow on urban arterial streets and its relationship with safety. Accident Analysis & Prevention, Volume 43, Issue 5, Pages 1610-1616.
7. Dixit, V.V. (2013). Behavioural foundations of two-fluid model for urban traffic. Transportation Research Part C, Volume 35, Pages 115-126.
8. Durr, C., Hoyer, P. (1996). A quantum algorithm for finding the minimum. arXiv preprint arXiv:quant-ph/9607014
9. Grover, L. K. (1997). A framework for fast quantum mechanical algorithms. arXiv:quant-ph/9711043.
10. Harikrishnafkumar, R.; Nannapaneni, S.; Nguyen, N. H.; Steck, J. E.; and Behrman, E. C. (2020) "A quantum annealing approach for dynamic multi-depot capacitated vehicle routing problem," arXiv preprint arXiv:2005.12478.
11. Hussain, H., Javaid, M.B., Khan, F.S. et al. (2020). Optimal control of traffic signals using quantum annealing. Quantum Inf Process 19, 312.
12. Kadowaki, T.; Nishimori, H. (1998) Quantum annealing in the transverse Ising model. Phys. Rev. E , 58, 5355.
13. Ligterink, N.E.; Kraan, T.C.; Eijk, A.R.A. (2012). Dependence on technology, drivers, roads, and congestion of real-world vehicle fuel consumption. Editor(s): Gaydon, Warwickshire, Sustainable Vehicle Technologies, Woodhead Publishing, 2012, Pages 123-134, ISBN 9780857094568, https://doi.org/10.1533/9780857094575.3.123.

14. Montanaro, A. (2016). Quantum algorithms: an overview. npj Quantum Inf 2, 15023.
15. Neukart, F.; Compostella, G.; Seidel, C.; Von Dollen, D.; Yarkoni, S.; Parney, B. (2017). Traffic flow optimization using a quantum annealer. Front. ICT , 4, 29.
16. Nielsen, M.A. and Chuang, I. L. (2011). Quantum Computation and Quantum Information: 10th Anniversary Edition (10th. ed.). Cambridge University Press, USA.
17. Papalitsas, Christos; Andronikos, Theodore; Giannakis, Konstantinos; Theocharopoulou, Georgia; Fanarioti, Sofia. (2019). A QUBO Model for the Traveling Salesman Problem with Time Windows. Algorithms 12, no. 11: 224. https://doi.org/10.3390/a12110224
18. Preskill, J. (2018). Quantum computing in the NISQ era and beyond. Quantum 2, 79.
19. Shor, P.W. (1994). "Algorithms for quantum computation: discrete logarithms and factoring". Proceedings 35th Annual Symposium on Foundations of Computer Science. IEEE Comput. Soc. Press: 124–134.
20. Simon, D.R. (1994). On the power of quantum computation. In: 35th FOCS. pp. 116–123. IEEE Computer Society Press (Nov 1994).
21. Warren, R. H. (2019). Solving the traveling salesman problem on a quantum annealer. SN Applied Sciences (2020) 2:75 | https://doi.org/10.1007/s42452-019-1829-x